Long term aging effect on the creep strength of the T92 steel

Clara Panait, Anne-Françoise Gourgues-Lorenzon, Jacques Besson, A. Fuchsmann, W. Bendick, J. Gabrel, M. Piette

LONG-TERM AGING EFFECT ON THE CREEP STRENGTH OF THE T92 STEEL

C. Panait[1,2], A.-F. Gourgues-Lorenzon[1], J. Besson[1], A. Fuchsmann[2], W. Bendick[3], J. Gabrel[2], M. Piette[2]

[1]Centre des Matériaux, MINES ParisTech, UMR CNRS 7633, B.P. 87, 91003 Evry Cedex, France
[2] V&M France CEV, Route de Leval, B.P. 20149, 59620 Aulnoye-Aymeries, France
[3]SZMF, Salzgitter Mannesmann Forschung GmbH, Ehinger Straβe 200, D-47259 Duisburg, Germany

Abstract

Creep strength loss of T92 steel after long-term creep exposure at 600°C and 650°C is partially due to a thermal aging of the steel during the first part of the test. In order to quantify the effect of long-term aging on the creep strength loss, creep tests were conducted at 600 and 650°C on T92 steel thermally aged for 10,000h at the same temperature and on as-received T92 steel.

Laves phases precipitates were found after thermal aging at 600°C and 650°C with an average equivalent diameter of about 200nm and of about 350nm, respectively. No significant change in hardness and in the matrix substructure as revealed by electron backscatter diffraction occurred during aging.

For stresses higher than 170MPa at 600°C and higher than 110MPa at 650°C the time to rupture is four times lower in the aged steels compared to the as-received steel, this is correlated to a secondary creep rate four times higher for the aged specimens compared to that of the as-received steel. Creep tests conducted at 650°C under lower stresses revealed a creep lifetime only twice lower after aging.

Keywords: creep, thermal aging, Grade 92 steel, Laves phases

1. Introduction

High temperature exposition causes a microstructural evolution, which could degrade the good mechanical proprieties of heat-resistant steels, such as creep strength. The effect of thermal aging on the creep strength degradation is most significant at high temperature (e.g. 600°C and 650°C) and during long-term creep exposure (times higher than 10^4h).

During long-term creep exposure or aging at 600°C and 650°C of 9-12%Cr heat resistant steels the following microstructural mechanisms were reported: precipitation of new secondary phases (Laves phases, Z-phase), growth of precipitates and recovery of the matrix (decrease in dislocation density inside subgrains, growth of subgrains) [1, 2]. Precipitation of Z-phase is much less intense in 9%Cr steels compared to 12%Cr steels [3], for which it is sometimes associated with premature loss of creep strength [4]. The main microstructural degradation mechanisms of 9%Cr heat resistant steels during long-term creep and/or aging are Laves phase precipitation and recovery of the matrix rather than precipitation of Z-phase [5].

After stress-free thermal aging at 600°C and 650°C for 10^4h some subgrain growth was reported in a 9% Cr tempered martensite steel [6] but the dominant microstructural evolution is precipitation of Laves phases. Nevertheless, the effect of microstructural evolution on the creep strength loss is not fully understood and there are still few quantitative data on the microstructure of 9-12%Cr heat resistant steels after long-term creep exposure.

The purpose of this study was to investigate the effect of prior thermal aging on the creep strength of the T92 steel. The steel was thermally aged at 600°C and 650°C for 10^4h in order to precipitate large Laves phases. Then creep tests were conducted at the same temperature as the aging heat treatments to study the effect of Laves phase precipitation on the loss of the creep strength and on creep damage development.

2. Experimental procedure

2.1 Materials and creep testing

The T92 steel investigated in this study was delivered by V&M Tubes France as a tube having 48.3mm outside diameter and 11.2 mm wall thickness. Its chemical composition and heat treatment are given in Table 1.

Table 1. *Chemical composition and heat treatment of the investigated T92 steel*

	Chemical Composition, wt. %													
	C	**Si**	**Mn**	**P**	**S**	**Al**	**Cr**	**Ni**	**Mo**	**V**	**Nb**	**W**	**N**	**B**
T92 steel	0.12	0.20	0.50	0.015	0.002	0.001	8.79	0.15	0.38	0.20	0.056	1.67	0.047	0.0026
Heat treatment : 1060°C for 20 min +780°C for 60 min														

During creep or thermal exposure at 600°C and 650°C of the 9-12%Cr heat resistant steels, there is a precipitation of Laves phases. A significant growth of Laves phases is observed during the first 10^4h of exposure followed by a slight increase for longer times [7]. Thus the duration of the aging heat treatments was chosen to be 10^4h in order to precipitate large Laves phases.

To this aim, full-thickness specimen blanks were cut parallel to the tube axis. Some of them were aged in induction furnaces at 600±2°C and 650°±2°C for 10^4h. The temperature during aging heat treatments was controlled with thermocouples welded on the samples.

Creep specimens with a gauge diameter of 5mm and a gauge length of 27mm were cut at mid-thickness from both as-received and aged materials and tested at 600°C and 650°C under levels of stress in the ranges 170-210MPa and 95-150MPa respectively. The purpose of creep tests on the as-received material was i) to compare the creep strength of the investigated T92 steel with available published creep rupture data for the Grade 92 steel and ii) to get reference samples for microstructural investigations to be further compared with aged T92 steel creep tested under the same conditions.

The secondary creep rate was estimated using simplified data processing of creep curves by assuming a heuristic decomposition of the creep strain as follows:

$$\varepsilon(t) = E_0 + Q\left(1 - \exp\left(\frac{t}{\tau}\right)\right) + \dot{\varepsilon}_{ss} t \qquad (1)$$

where t is time in hours; E_0 is the instantaneous elastic/plastic strain due to loading; Q and τ are fitting parameters characterizing the primary creep stage and $\dot{\varepsilon}_{ss}$ is taken as the secondary creep rate. The value of $\dot{\varepsilon}_{ss}$ was determined by fitting equation 1 up to half the creep lifetime of each specimen.

2.2 Microstructural characterization

Microstructural characterization was realized using Scanning Electron Microscopy (SEM), Electron Backscatter Diffraction (EBSD) techniques and hardness measurements. All investigations were conducted on mid-thickness longitudinal cross-sections.

Because Laves phase are relatively large particles, average equivalent diameter larger than 150 nm, SEM techniques are best suitable to study growth and coarsening of these

phases during creep exposure compared to transmission electron microscopy techniques [8]. Due to their chemical composition, Laves phases can be easily revealed as bright precipitates in a dark matrix using backscatter electron (BSE) imaging, whereas $M_{23}C_6$ carbides have lower average atomic number compared to that of the matrix. Thus all bright precipitates in such images are Laves phases. The size distribution of Laves phases was thus determined in aged samples by analysis of SEM-BSE images acquired after a final mechanical-chemical polishing with colloidal silica. For each sample almost forty images with a magnification of 2000 were analyzed and thousands of particles were quantified.

To investigate matrix recovery, EBSD investigations of the steel microtexture were conducted on the aged T92 samples after a final polishing with colloidal silica. EBSD maps were acquired with a step size of 0.15 µm, high voltage 20kV, working distance 19 mm, aperture 120 µm, probe current between 0.1 and 1nA using a Zeiss DSM 982 Gemini field emission gun (FEG) SEM equipped with a Shottky filament together with a Hjelen-type camera and TSL OIM facilities.

Creep damage was investigated using SEM on longitudinal cross-sections of the crept specimens in the gauge length after final mechanical-chemical polishing with colloidal silica.

3. Microstructural characterization of the thermally aged material

3.1 Hardness

No significant change in hardness was observed after aging at 600°C and 650°C for 10^4h: 231 ±3 $HV_{0.5}$ for the as-received material, 236 ±4 $HV_{0.5}$ and 232±4 $HV_{0.5}$ for the material aged at 600°C and 650°C, respectively.

3.2 Size of Laves phases

The size distribution of Laves phases follow a lognormal distribution with an average equivalent diameter of ~250nm and of ~350nm in specimens thermally aged at 600°C and 650°C, respectively (Figure 1). This is consistent with literature data [8]. Typical images used for the quantification of Laves phases are shown in Figure 2.

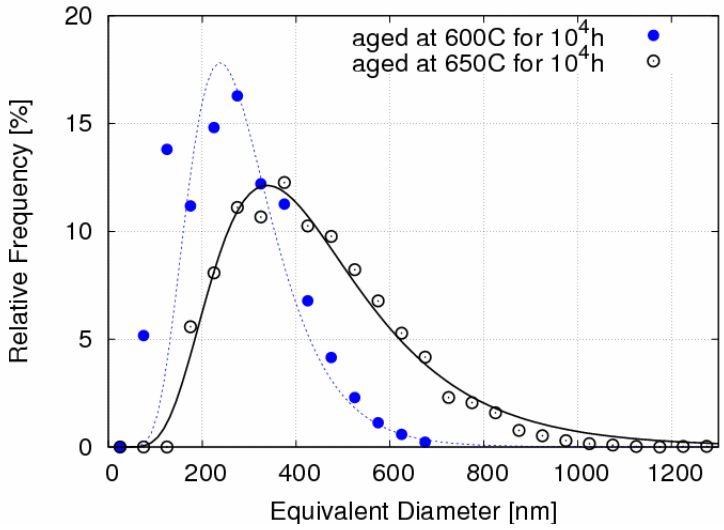

Figure 1 *Size distribution of Laves phases in the T92 aged steels determined by image analysis of SEM-BSE images (symbols) compared with a lognormal fit (lines)*

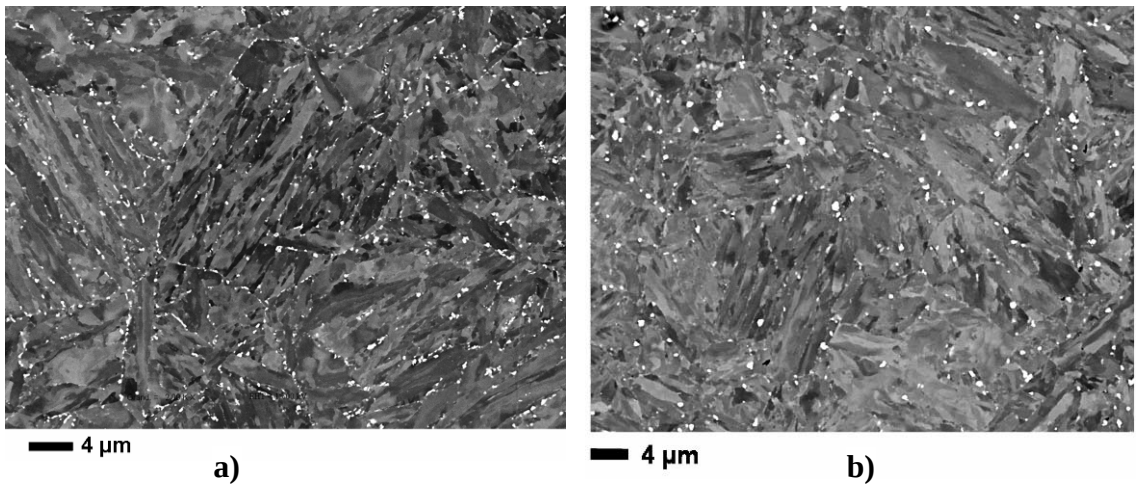

Figure 2 *Typical SEM-BSE images used for quantification of Laves phases a) T92 steel aged at 600°C for 10^4h; b) T92 steel aged at 650°C for 10^4h*

3.3 Microtexture

EBSD maps revealed no significant change in the microtexture after aging at 600°C and 650°C (Figures 3-5). All inverse pole figure (IPF) and image quality maps showed typical tempered martensite with blocks and packets. This is confirmed by the histograms of boundary misorientation angles (Figure 6) showing a typical distribution of boundaries between martensite variants formed from the same parent austenite grain [9, 10]. Only a slight decrease in the amount of low angle boundaries is observed after aging both at 600°C and 650°C.

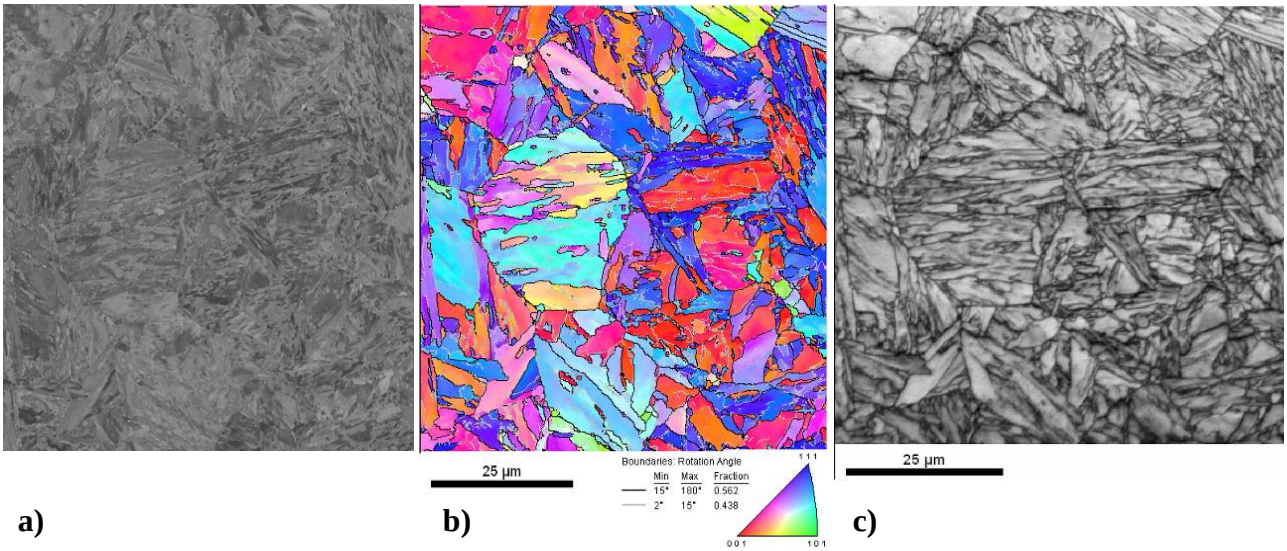

Figure 3 *Microstructure of the as-received T92 steel. a) BSE image; b) EBSD IPF map with orientation of sample normal in the crystal frame as colour key; c) EBSD image quality map*

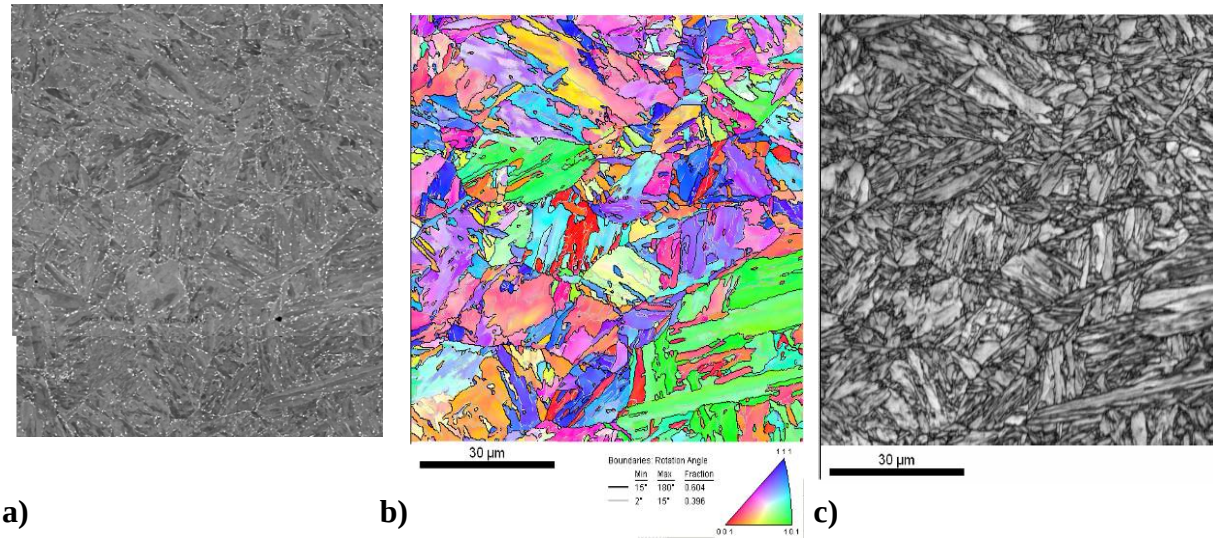

Figure 4 *Microstructure of the T92 steel aged at 600°C for 10^4h. a) BSE image; b) EBSD IPF map (same colour key as in Figure 3b); c) EBSD image quality map*

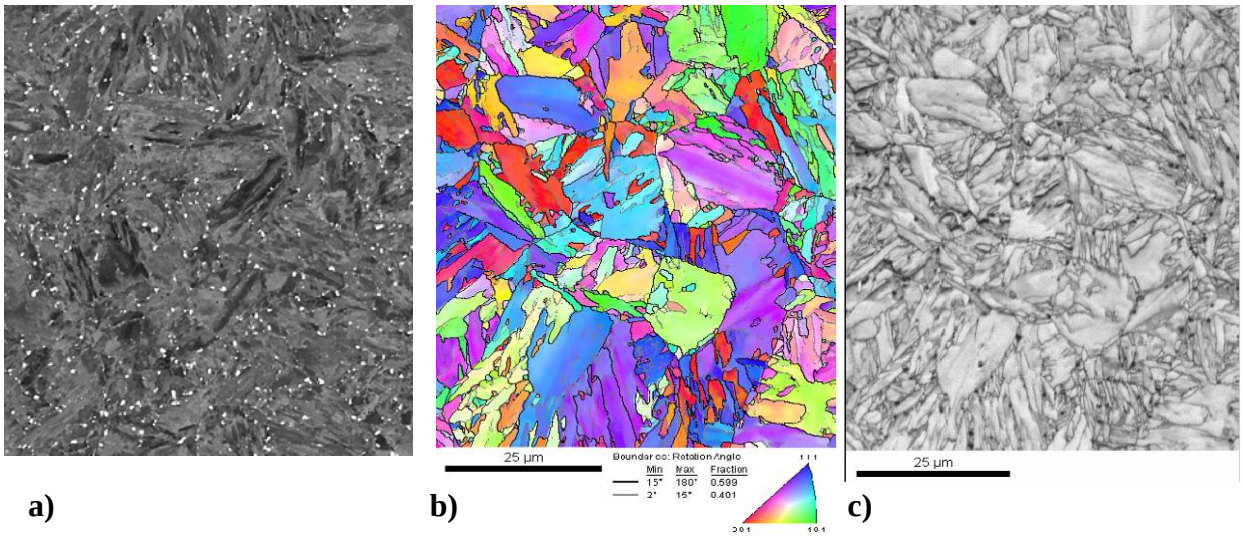

Figure 5 *Microstructure of the T92 steel aged at 650°C for 10^4h. a) BSE image; b) EBSD IPF map (same colour key as in Figure 3b); c) EBSD image quality map*

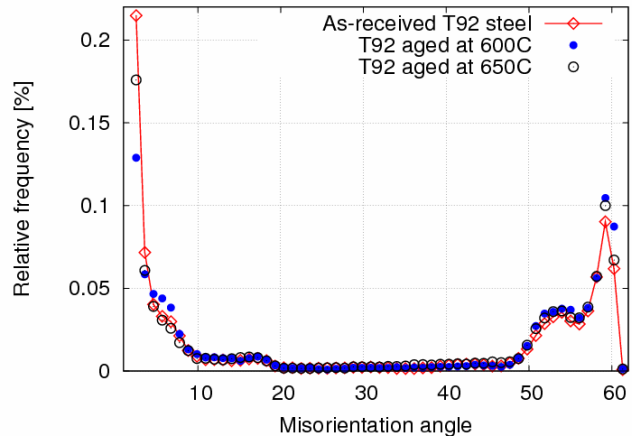

Figure 6 *Boundary misorientation angle distributions from EBSD maps shown in figures 3-5*

4. Results of creep tests

4.1 Effect of thermal aging at 600°C for 10^4h

After aging at 600°C for 10^4h the T92 steel shows a higher secondary creep rate ($\dot{\varepsilon}_{ss}$) and a lower time to rupture (divided by about 3) compared to the as-received T92 steel for the same testing conditions (Figures 7-8 and Table 2). The increase in $\dot{\varepsilon}_{ss}$ after aging might be attributed to the precipitation of Laves phases, which depletes the matrix of W and Mo atoms in solid solution. Thermal aging at 600°C for 10^4h does not seem to significantly influence the creep ductility of the T92 steel in the investigated conditions.

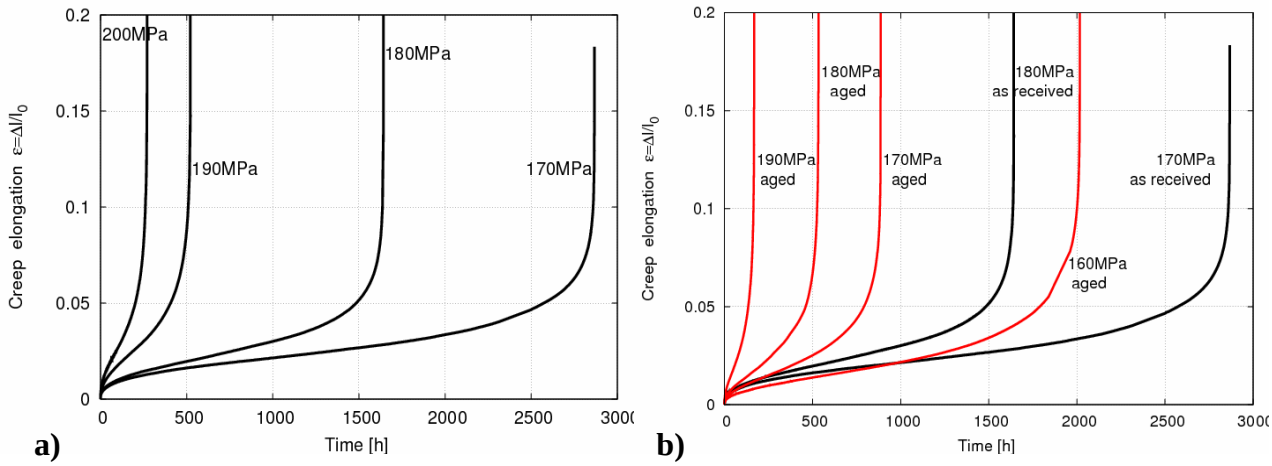

Figure 7 *Creep curves at 600°C. a) As-received material, b) material aged at 600°C for 10^4h*

Table 2 *Creep results at 600°C (A: fracture elongation; Z: reduction in area)*

	As-received T92 steel					T92 steel aged at 600°C for 10^4h				
Temp. [°C]	Stress [MPa]	Time [h]	*A* [%]	*Z* [%]	$\dot{\varepsilon}_{ss}$ [10^{-5} h^{-1}]	Stress [MPa]	Time [h]	*A* [%]	*Z* [%]	$\dot{\varepsilon}_{ss}$ [10^{-5} h^{-1}]
600	210	112	28.7	89	43.8	-	-	-	-	-
	200	270	29.8	90	17.4	-	-	-	-	-
	190	523	28.4	85	8.6	190	169	26.7	87	25.3
	180	1642	23.2	84	2.1	180	534	26.2	87	7.3
	170	2867	21.0	78	1.1	170	886	21.6	82	3.9
	-	-	-	-	-	160	2016	24.1	82	1.6

The ECCC regression line in figure 8b was taken from reference [11]. The creep results of the as-received T92 steel are comparable with results commonly reported for the Grade 92 steel.

The stress dependence of $\dot{\varepsilon}_{ss}$ was modelled by a Norton power law, (equation 2), where *B* and *n* are temperature-dependent constants; the value of σ_0 was arbitrarily set to 100MPa. From the creep results at 600°C it was found $B= 0.05\times10^{-8}h^{-1}$ and n=18 for the as-received T92 steel and $B= 0.21\times10^{-8}h^{-1}$ and n=18 for the thermally aged T92 steel.

$$\dot{\varepsilon}_{ss} = B\left(\frac{\sigma}{\sigma_0}\right)^n \qquad (2)$$

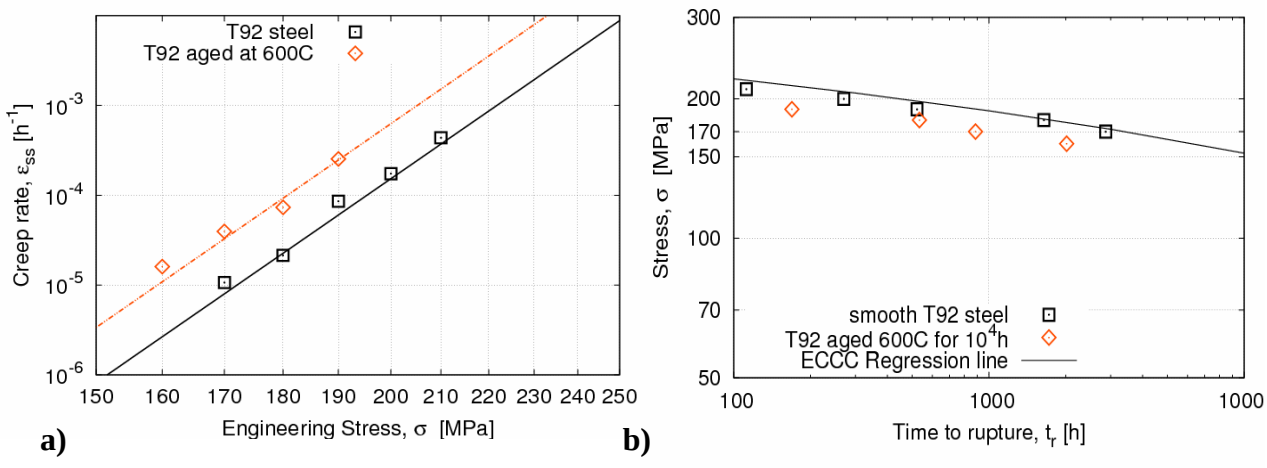

Figure 8 *Secondary creep rate (a) and time to rupture (b) as a function of engineering stress at 600°C. Symbols: experimental results; lines in (a): fit using a Norton flow rule*

4.2 Effect of thermal aging at 650°C for 10^4h

The results of creep at 650°C are summarized in Table 3 and Figure 9. Relatively high values of reduction of area (Z) and fracture elongation (A) are observed for creep lifetime lower than 1000h, indicating failure by viscoplastic instability (necking). For longer lifetimes, another damage mechanism is expected to occur.

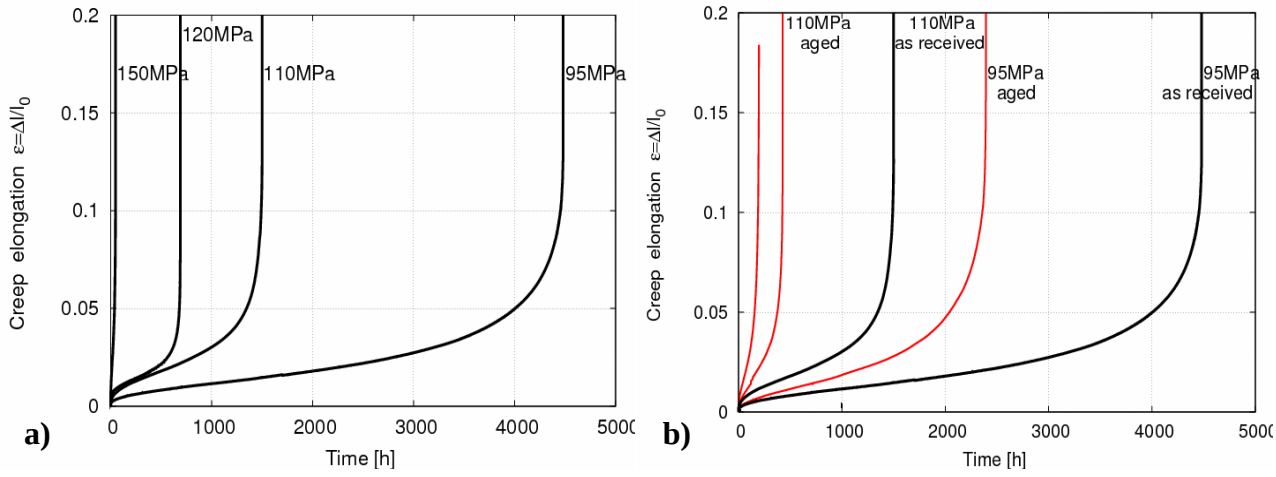

Figure 9 *Creep curves at 650°C. a) As-received material, b) material aged at 650°C for 10^4h*

Creep tests conducted on the T92 steel thermally aged 650°C for 10^4h revealed a lower time to rupture and a higher $\dot{\varepsilon}_{ss}$ compared to the as-received T92 steel for the same testing conditions. The difference between the values of $\dot{\varepsilon}_{ss}$ of the as-received T92 steel and those of

aged T92 steel depends on the level of applied stress. Compared to the as received T92 steel for same testing conditions the $\dot{\varepsilon}_{ss}$ of the aged T92 steel is four times higher for levels of stress higher than 110MPa and only twice higher for levels of stress lower than 110MPa.

Table 3 *Creep results at 650°C (A: fracture elongation; Z: reduction in area)*

	As-received T92 steel					**T92 steel aged at 650°C for 10^4h**				
Temp. [°C]	Stress [MPa]	Time [h]	*A* [%]	*Z* [%]	$\dot{\varepsilon}_{ss}$ [10^{-5} h^{-1}]	Stress [MPa]	Time [h]	*A* [%]	*Z* [%]	$\dot{\varepsilon}_{ss}$ [10^{-5} h^{-1}]
650	150	50	26.3	92	95.7	-	-	-	-	-
	140	77	17.8	88	82.8	-	-	-	-	-
	120	691	26.1	84	2.5	120	199	33.7	88	21.1
	110	1502	22.9	77	2.1	110	427	20.6	80	9.4
	95	4480	14.9	35	0.6	95	2392	19.8	65	1.4
	-	-	-	-	-	85	4434	15.3	43	0.7

A change in slope is observed when plotting $\dot{\varepsilon}_{ss}$ as a function of stress both for as-received and aged materials (Figure 10). Two regions can be distinguished: high stresses (σ>110MPa) and low stresses (σ<110MPa). For each region the dependence of $\dot{\varepsilon}_{ss}$ upon applied stress can be described by a Norton power-law equation (equation 2). In equation 2 σ_0 was also set to 100MPa. For high stresses it was found B=1.07×10^{-6}h^{-1} and n=18 and for low stresses it was found B= 9.78×10^{-6}h^{-1} and n=6. A Norton law with B=4.06×10^{-6}h^{-1} and n=18 for high stresses and B=19.6×10^{-6}h^{-1} and n=6 for low stresses well represents the results of creep tests conducted on the T92 steel aged at 650°C for 10^4h.

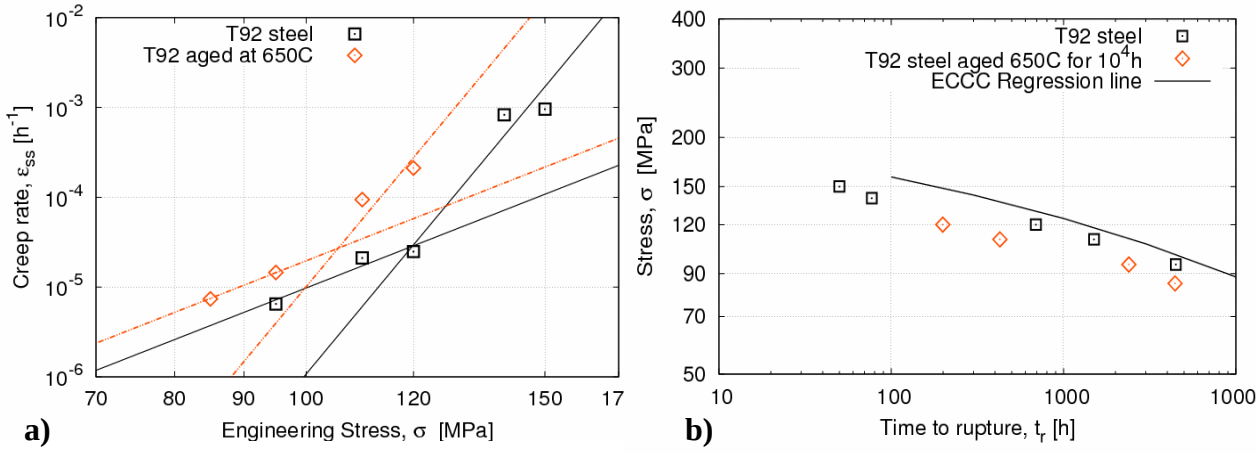

Figure 10 *Secondary creep rate (a) and time to rupture (b) as a function of engineering stress at 650°C. Symbols: experimental results; lines in (a): fit using a Norton flow rule*

The adjusted values of the Norton exponent are very high compared to the well-known theoretical values but they correspond to the values reported in literature for the creep flow of the Grade 92 steel [1, 12]. This is probably mainly due to the absence of a threshold stress in equation 2. Thus, the apparent change in Norton exponent could be due to a change in internal stresses during long-term creep testing rather than to a change in the dominant creep

mechanism. Moreover, the low number of tests conducted here at low stresses does not allow accurate estimation of the Norton law exponent in the low stress region. No evidence of diffusional creep has so far been reported in the Grade 92 steel, in contrast with Grade 91 steel [13, 14].

5. Investigations of the crept specimens

Creep damage investigations conducted on longitudinal cross sections of the crept specimens tested at 600°C revealed cavities only on the necking area. Stress triaxiality due to necking at the end of specimen lifetime could have caused nucleation and growth of these cavities. No creep damage was observed on the part of the specimens homogeneously deformed during the creep test.

In specimens of both as-received and aged T92 steel tested at 650°C for times lower than 1000h, cavities were observed only in the necking area. Scarcely distributed creep damage cavities (typically a few μm in size) were observed in all the gauge part of the crept specimens tested for times higher than 4000h (Figure 11).

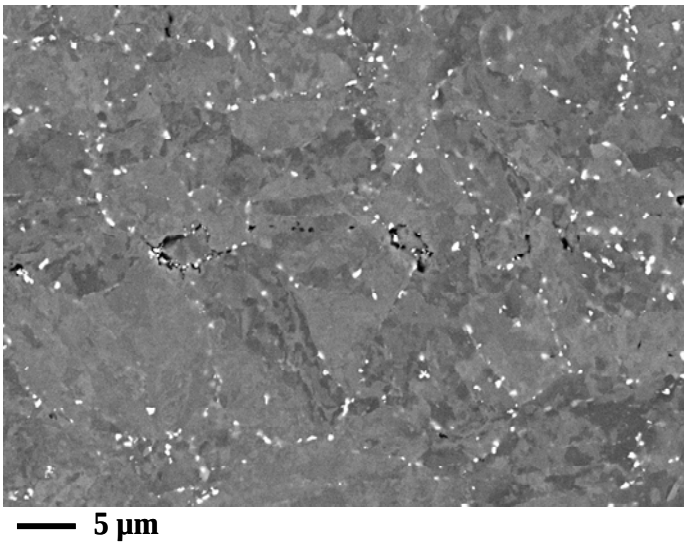

Figure 11 *Creep damage cavities (in black) observed with SEM-BSE in the homogeneously deformed part of the specimen of as-received steel crept at 650°C for 95 MPa*

6. Summary and conclusions

The most obvious change in the microstructure of the T92 steel after aging was the significant precipitation of Laves phases. In this study no significant evolution of the matrix during aging heat treatments was observed using EBSD. Complementary transmission electron microscopy observation could be made to clarify this point. This is beyond the scope of the present study, which focuses on Laves phases.

After aging an increase in secondary creep rate ($\dot{\varepsilon}_{ss}$) is observed. At 650°C this increase depends on the level of applied stresses. Creep tests conducted at 600°C on both as-received T92 steel and T92 steel aged at 600°C revealed a $\dot{\varepsilon}_{ss}$ four times higher in the aged T92 steel. Anyway the levels of stress investigated at 600°C were in the range 170-210MPa, which is relatively high and corresponds to the high stress region of the Grade 92 steel at

600°C [1, 13]. The difference between the $\dot{\varepsilon}_{ss}$ of the as-received T92 steel and T92 steel aged at 600°C might also decrease with decreasing the applied stress, as is the case at 650°C. This is also suggested by literature results on P92 steel aged at 650°C for 10^4h and then creep tested at 600°C [12].

Aging does not seem to significantly influence on creep damage development in the investigated conditions. Low amounts of creep damage was observed in crept specimens in as-received T92 steel and T92 steel aged at 650°C tested for times higher than 4000h.

References

1. Ennis P.J., Zielińska-Lipiec A., Wachter O., Czyrska-Filemonowicz A., Microstructure stability and creep rupture strength of the martensitic steel P92 for advanced power plant, *Acta Mater.* 45 (1997) 4901-4907

2. Seung Lee J., Armaki H. Gh., Maruyama K., Muraki T., Asahi H., Causes of breakdown of creep strength in 9Cr-1.8W -0.5Mo-VNb steel, *Mater. Sci. Eng. A* 428 (2006) 270-275

3. Danielsen H., Hald J., Behaviour of Z phase in 9-12%Cr steels, *Energy Materials* 1 (2006), 49-57

4. Danielsen H., Hald J., A thermodynamic model of the Z-phase Cr(V,Nb)N, *Computer coupling of phase diagrams and thermochemistry* 31 (2007) 505-514

5. Panait C., Bendick W., Fuchsmann A., Gourgues-Lorenzon A.-F., Besson J., Study of the microstructure of the Grade 91 steel after more than 100,000h of creep exposure at 600°C, *Proc. "Creep & Fracture in high temperature components: Design & life assessment issues (ECCC Creep Conference);* 877-888, London, UK. Lancaster, PA: DEStech Publications. ISBN 978-1-60595-005-1

6. Ghassemi-Armaki H., Chen R.P., Maruyama K., Yoshizawa M., Igarashi M., Static recovery of tempered lath martensite microstructures during long-term aging in 9–12% Cr heat resistant steels, *Materials Letters* 63 (2009) 2423-2425

7. Dimmler G., Weinert P., Kozeschnik E., Cerjak H., Quantification of Laves phase in advanced 9-12%Cr steels using a standard SEM, *Mater. Charact.* 51 (2003) 341- 352

8. Korcakova L., Hald J., Somers A. J., Quantification of Laves phase particle size in 9CrW steel, *Mater. Charact.*, 47 (2001), 111-117

9. Morito S., Huang X., Furuhara T., Maki T., Hansen N., The morphology and crystallography of lath martensite in alloy steels, *Acta Mater.* 54 (2006) 5323-5331

10. Gourgues, A.-F., Flower H. M. and Lindley T.C., Electron backscattering diffraction study of acicular ferrite, bainite and martensite microstructure, *Mater. Sci. Technol.* 16 (2000) 26-40

11. Yoshizawa M., Igarashi M., Moriguchi K., Iseda A., Armaki H. G., Maruyama K., Effect of precipitates on long-term creep deformation properties of the P92 and P122 type advanced ferritic steels for USC power plant, *Mater. Sci. Eng. A* 510-511 (2009) 162-169

12. Sklenička V., Kuchařová K., Svoboda M., Kloc L., Buršík J., Kroupa A., Long-term creep behavior of 9–12%Cr power plant steels, *Mater. Charact* .51 (2003) 35-48

13. Kloc L., Sklenička V., Confirmation of low stress creep regime in 9% chromium steel by stress change creep experiments, *Mater. Sci. Eng. A,* 387-389 (2004) 633-638

14. Kloc L., Sklenička V., Transition from power-law to viscous creep behaviour of p-91 type heat-resistant steel, *Mater. Sci. Eng. A* 234-236, (1997) 962-965